STATE OF WASHINGTON
DEPARTMENT OF NATURAL RESOURCES
BRIAN J. BOYLE, Commissioner of Public Lands
JAMES A. STEARNS, Department Supervisor

DIVISION OF GEOLOGY AND EARTH RESOURCES
Raymond Lasmanis, State Geologist

SEDIMENTARY THICKNESS IN THE PUGET SOUND AREA, WASHINGTON

DERIVED FROM AEROMAGNETIC DATA

by

Z. F. Danes
Danes Research Associates
4206 N. 13th
Tacoma, WA 98406

Washington Department of Natural Resources
Division of Geology and Earth Resources
Olympia, WA 98504

Open-File Report 85-5

September 1985

Sedimentary Thickness in the Puget Sound Area, Washington, Derived from Aeromagnetic Data

Z.F. Daneš
Daneš Research Associates
4206 N. 13th
Tacoma, WA 98406
(206) 752-0600

Abstract

Since short wave harmonic components of the magnetic (or gravity) field decrease with elevation faster than the long wave components, profiles across anomalies become "smoother" with greater vertical separation between the level of magnetized rocks and the plane of observation.

Since igneous basement rocks are magnetic, while overlying sediments are not, differences between a magnetic profile across a basement outcrop and across a sedimentary basin may be used for determination of thickness of sedimentary layers.

The method has been used on the magnetic anomalies in the Puget Sound area and depth estimates are in good agreement with estimates derived from gravity anomalies.

Introduction

It is a well-known fact that, as a rule, igneous rocks have a comparatively high magnetic susceptibility and/or remnant magnetization, whereas sediments have neither (e.g., Nettleton, 1940). If from the analysis of magnetic data obtained either at ground level or from an aeromagnetic survey carried out at a height h, we can determine the depth to the magnetized horizon, we have for all practical purposes determined the thickness of the sedimentary section (unless, of course, a magnetized layer such as a lava flow within the sedimentary column is mistaken for the igneous basement).

This report presents a simple and reasonably accurate method that enables us to make such estimates (Daneš, 1962).

Theory

The magnetic intensity, $\vec{H}$, must satisfy three of Maxwell's equations:

$$\vec{\Delta}\cdot(\mu\vec{H}) = 0 \ , \tag{1}$$

$$(\partial/\partial t)(\mu\vec{H}) = -\vec{\Delta} \times \vec{E} \ , \tag{2}$$

$$\vec{\Delta} \times \vec{H} = (\partial/\partial t)(\varepsilon\vec{E}) + g\vec{E} \ , \tag{3}$$

where

μ = magnetic permeability

ε = electric permittivity

g = electric conductivity

$\vec{E}$ = electric field

t = time

Since measurements are carried out in the air, where ε and μ are constant and $g = 0$; since further, the magnetic and electric fields are almost constant in time, (2) is irrelevant, and (1) and (3) reduce to

$$\vec{\Delta} \cdot \vec{H} = 0 \qquad (4)$$

$$\vec{\Delta} \times \vec{H} = 0 \qquad (5)$$

Then $\vec{H}$ has a scalar potential, U, such that

$$\vec{H} = -\vec{\Delta}U \qquad (6)$$

and U is harmonic:

$$\Delta^2 U = 0 \ . \qquad (7)$$

But then, too, any directional derivative of U, and therefore any Cartesian component of $\vec{H}$ is harmonic:

$$\Delta^2 H_s = 0 \tag{8}$$

where H_s is the component of the $\vec{H}$ vector in the s-direction.

It should be mentioned here that the same is not true about the total magnetic intensity, $|\vec{H}|$, since

$$\left|\vec{H}\right| \equiv \sqrt{H_x^2 + H_y^2 + H_z^2} = \sqrt{(\partial U/\partial x)^2 + (\partial U/\partial y)^2 + (\partial U/\partial z)^2} \tag{9}$$

$|\vec{H}|$ does not satisfy (8), as can be shown by direct substitution. Fortunately nevertheless, the perturbations of the field are small compared with the main ambient field. Then the total field is almost equal to its projection into the average, "unperturbed" vector direction, and we can say that

$$\Delta^2 |\vec{H}| \simeq 0 \tag{10}$$

in most cases. ($|\vec{H}|$ varies between 30,000 and 70,000 gamma, while an anomaly of 3,000 gamma is considered strong; even if the anomalous field were perpendicular to the unperturbed field,

$$\sqrt{30{,}000^2 + 3{,}000^2} = 30{,}150 ,$$

so that the error amounts to only one-half percent.)

The solution of (10) can be written as a two-dimensional Fourier series,

$$\left|\vec{H}\right| = \sum_m \sum_n A_{mn} \cdot \begin{pmatrix}\cos\\ \sin\end{pmatrix} 2\pi m \frac{x}{\ell} \cdot \begin{pmatrix}\cos\\ \sin\end{pmatrix} 2\pi n \frac{y}{\ell} \cdot e^{-2\pi\sqrt{m^2+n^2}\,\frac{z}{\ell}} \tag{11}$$

where x and y are horizontal coordinates, z is vertical, m and n are integers, ℓ is a distance large enough (greater than horizontal extent of magnetic anomalies) so that the field may be treated as periodic, and A_{mn} are coefficients to be determined by the Fourier analysis.

We see from (11) that with increasing z, all harmonic components are attenuated; however they are not attenuated at the same rate, shorter wavelengths being attenuated more, while longer ones are attenuated less.

Procedure

We now can proceed as follows: start with a typical profile (or several profiles) across a known outcrop of basement rocks; Fourier analyze this profile; since the profile has been flown at an elevation h, the coefficients of the expansion are

$$A_{mn} \cdot e^{-2\pi\sqrt{m^2+n^2}\,\frac{h}{\ell}}$$

Unless there is a conspicuous preferential orientation of the anomalies, we may assume that m = n, and the Fourier analysis then yields coefficients

$$A_m \cdot e^{-2\pi m\sqrt{2}\,\frac{h}{\ell}}$$

Next, we recalculate the coefficients of those test profiles for various depths; e.g., 0.5 km, 1 km, 2 km, 4 km, etc., and draw those profiles. Finally we compare those test profiles with other profiles constructed at

different parts of the sedimentary basin, and look for similarities. In particular, we look for the vanishing short wave components. Assuming then that the difference between the profile at the outcrop and the profile over the sediments is due only to the greater distance to the magnetic rocks, we have found the thickness of the sediments.

Figures 1 through 7 illustrate the procedure on a profile taken over the Crescent Volcanics of the northern Olympic Peninsula. Table I gives the observed values at an elevation of about 1 km (3,000 ft) and derived residual values at other elevations. Table II gives the coefficients of the Fourier expansion at corresponding values of z.

The attached map (reduced and reproduced as Figure 8) is a map of the Puget Sound area, East and North shore of the Olympic Peninsula and Strait of Juan de Fuca. It is based on the Preliminary Aeromagnetic Map of the Puget Sound Area, Washington, scale 1:125,000, U.S. Geological Survey, 1974 (reduced and reproduced as Figure 1). The circles are midpoints of profiles used for the estimates, and numerical values are estimated sedimentary thicknesses in km. Isopacks were drawn as if those thicknesses represented a continuous function, rather than a geological feature full of discontinuities, such as faults and pinch outs. Results are in good agreement with estimates based analysis of gravity anomalies (Daneš et al., 1965).

It is expected that results could be greatly improved if the person carrying out the analysis had an adequate geological education, or worked in concert with an experienced geologist.

Bibliography

Daneš, Z.F., 1962, Structure calculation from gravity data and density logs: Trans. Soc. Mining Engineers, v. 1, p. 23-29.

Daneš, Z.F., et al., 1965, Geophysical investigation of the Southern Puget Sound Area, Washington: J. Geophys. Research, v. 70, p. 5573.

Nettleton, L.L., 1940, Geophysical prospecting for oil: McGraw-Hill, New York, p. 203.

U.S. Geological Survey, 1974, Aeromagnetic map of part of the Puget Sound area, Washington: U.S. Geological Survey Open-File Report 74-1106, 1 sheet, scale 1:125,000.

Table I.
Profile A-A' continued to different depths.

z = 0	z = 1 km	z = 2 km	z = 3 km	z = 5 km	z = 6 km	z = 8 km	z = 11 km
- 4,998	5,060	- 514	-126	35	38	21	2
- 1,107	6,500	- 10	46	57	44	20	0
4,999	8,430	558	247	83	51	17	- 2
8,635	8,250	653	333	95	50	10	- 6
-11,424	6,630	462	306	80	35	- 1	-10
9,534	7,825	471	233	36	3	-17	-15
- 1,885	7,750	336	81	- 35	- 42	-36	-21
6,386	7,060	- 144	-179	-120	- 93	-55	-25
- 5,651	5,000	- 824	-468	-201	-140	-72	-29
- 9,160	4,000	-1,154	-635	-256	-172	-82	-30
1,681	5,700	- 921	-627	-273	-182	-83	-29
1,540	6,180	- 672	-543	-253	-167	-74	-24
- 4,515	6,210	- 607	-465	-200	-129	-55	-18
11,425	5,750	- 726	-373	-116	- 71	-29	- 9
-29,107	3,510	- 601	-143	- 4	2	2	0
18,216	8,105	420	275	122	78	32	10
- 364	9,270	1,274	672	231	142	57	18
6,363	9,680	1,562	857	293	179	73	24
7,716	9,160	1,352	798	291	182	78	28
- 5,930	7,300	818	574	232	151	71	29
3,405	7,350	441	291	133	96	56	29
472	7,370	44	- 37	16	31	37	27
6,461	6,220	- 689	-413	- 90	- 27	20	25
-12,692	2,980	-1,517	-706	-155	- 61	11	24

(All values in gamma)

Table II.
Coefficients of expansion,
Profile A-A'

	z = 0	z = 1 km	z = 2 km	z = 3 km	z = 5 km	z = 6 km	z = 8 km	z = 11 km
a_1	− 108.96	− 93.96	− 81.03	− 69.87	+ 51.96	−44.81	−33.32	−21.37
a_2	+ 445.98	+ 331.65	+246.58	+183.41	+101.42	+75.42	+41.71	+17.15
a_3	+1,345.43	+ 862.80	+553.30	+354.82	+145.92	+93.57	+38.48	+10.15
a_4	−2,894.92	−1,600.92	−885.32	−489.72	−149.72	−82.80	−25.32	− 4.28
a_5	+ 321.99	+ 153.55	+ 73.23	+ 34.92	+ 7.94	+ 3.79	+ 0.86	+ 0.09
a_6	−1,342.04	− 551.90	−226.96	− 93.34	− 15.78	− 6.49	− 1.10	− 0.08
a_7	− 918.33	− 325.67	−115.49	− 40.96	− 5.15	− 1.83	− 0.23	− 0.01
a_8	+ 667.85	+ 204.24	+ 62.46	+ 19.10	+ 1.79	+ 0.55	+ 0.05	0
a_9	+ 798.27	+ 210.52	+ 55.52	+ 14.64	+ 1.02	+ 0.27	+ 0.02	0
a_{10}	−5,485.47	−1,247.50	−283.71	− 64.52	− 3.34	− 0.76	− 0.04	0
a_{11}	− 54.41	− 10.67	− 2.09	− 0.41	− 0.02	0	0	0
a_{12}	− 871.04	− 147.31	− 24.91	− 4.21	− 0.12	− 0.02	0	0
a_{13}	+ 535.93	+ 78.16	+ 11.40	+ 1.66	+ 0.04	+ 0.01	0	0
a_{14}	− 767.55	− 96.53	− 12.14	− 1.53	− 0.02	0	0	0
a_{15}	+3,249.34	+ 352.40	+ 38.22	+ 4.14	+ 0.05	+ 0.01	0	0
a_{16}	− 891.00	− 83.33	− 7.79	− 0.73	− 0.01	0	0	0
a_{17}	− 822.81	− 66.36	− 5.35	− 0.43	0	0	0	0
a_{18}	+5,240.37	+ 364.46	+ 25.35	+ 1.76	+ 0.01	0	0	0
a_{19}	+2,416.34	+ 144.92	+ 8.69	+ 0.52	0	0	0	0
a_{20}	−7,290.11	− 377.04	− 19.50	− 1.01	0	0	0	0
a_{21}	+1,776.45	+ 79.23	+ 3.53	+ 0.16	0	0	0	0
a_{22}	+ 514.29	+ 19.78	+ 0.76	+ 0.03	0	0	0	0
a_{23}	−5,902.92	− 195.78	− 6.49	− 0.22	0	0	0	0
a_{24}	0	0	0	0	0	0	0	0

(All values in gamma)

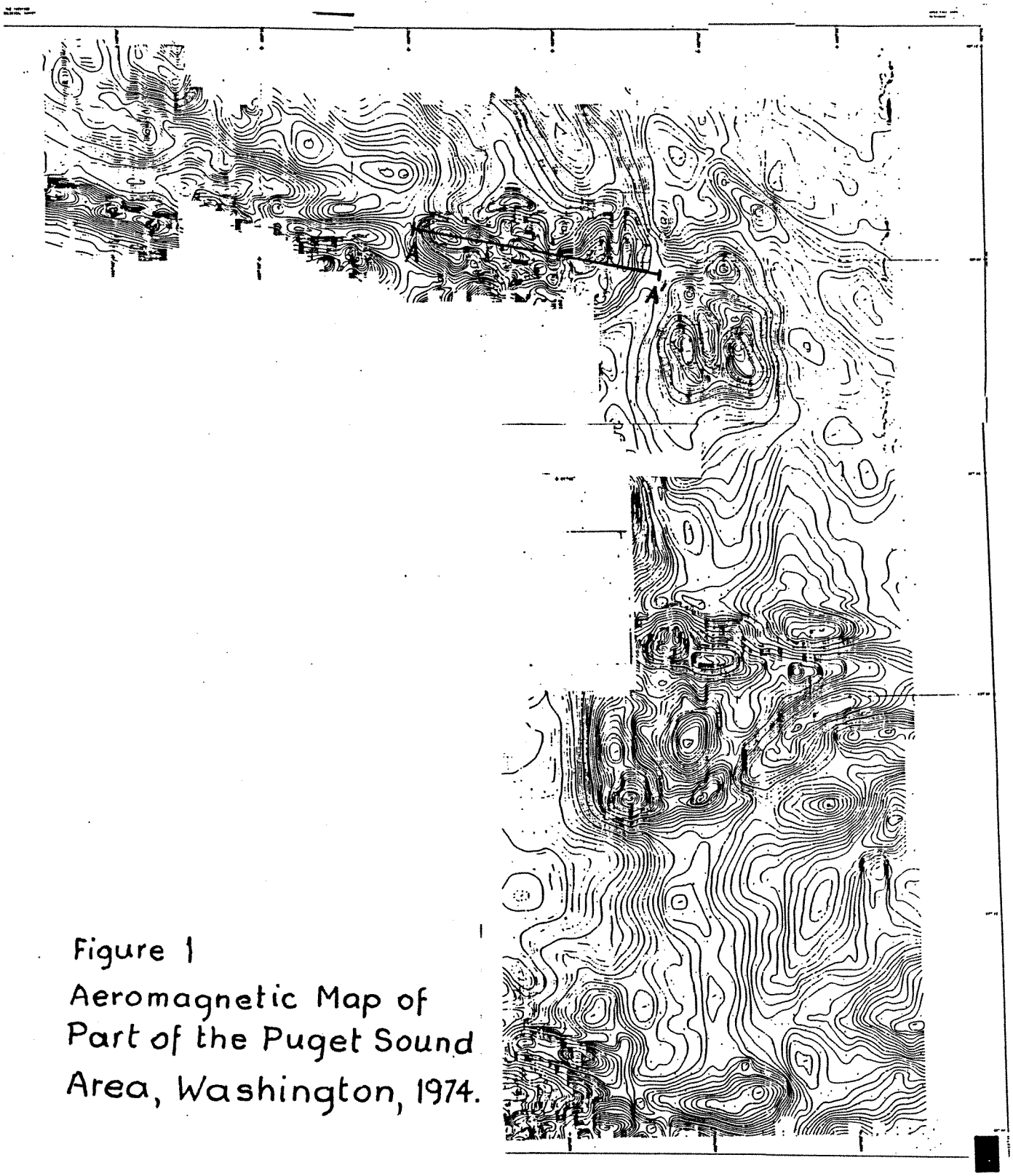

Figure 1
Aeromagnetic Map of
Part of the Puget Sound
Area, Washington, 1974.

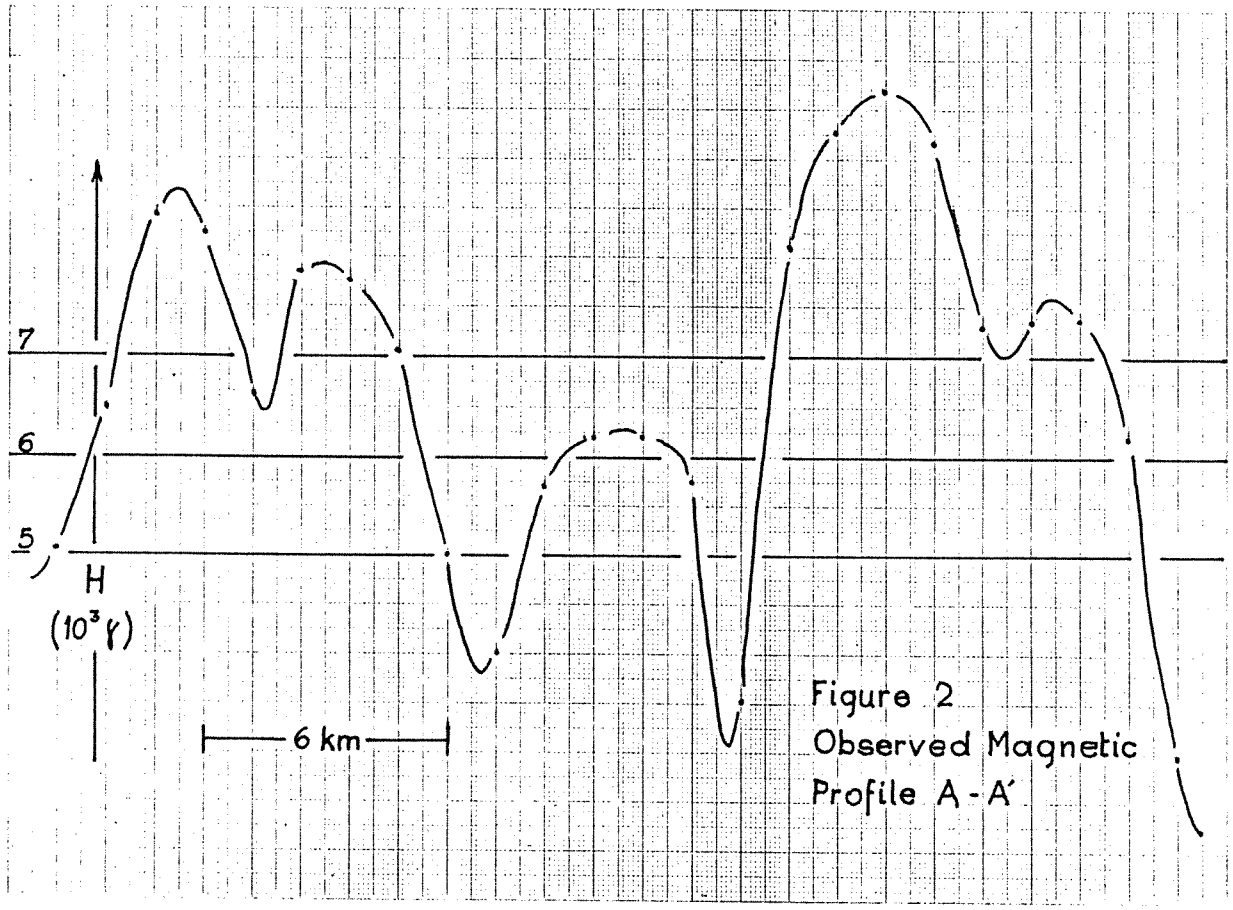

Figure 2
Observed Magnetic
Profile A - A'

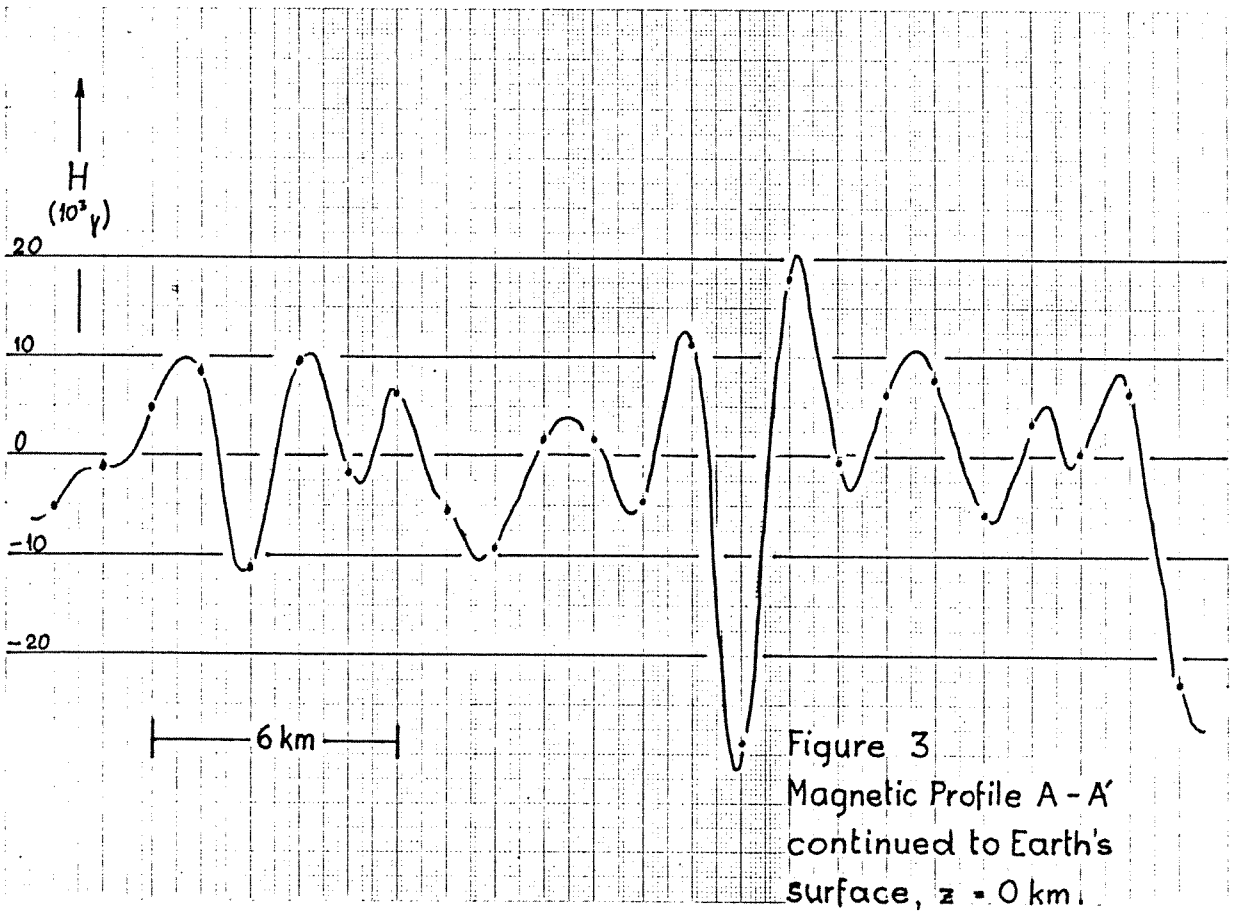

Figure 3
Magnetic Profile A - A'
continued to Earth's
surface, z = 0 km.

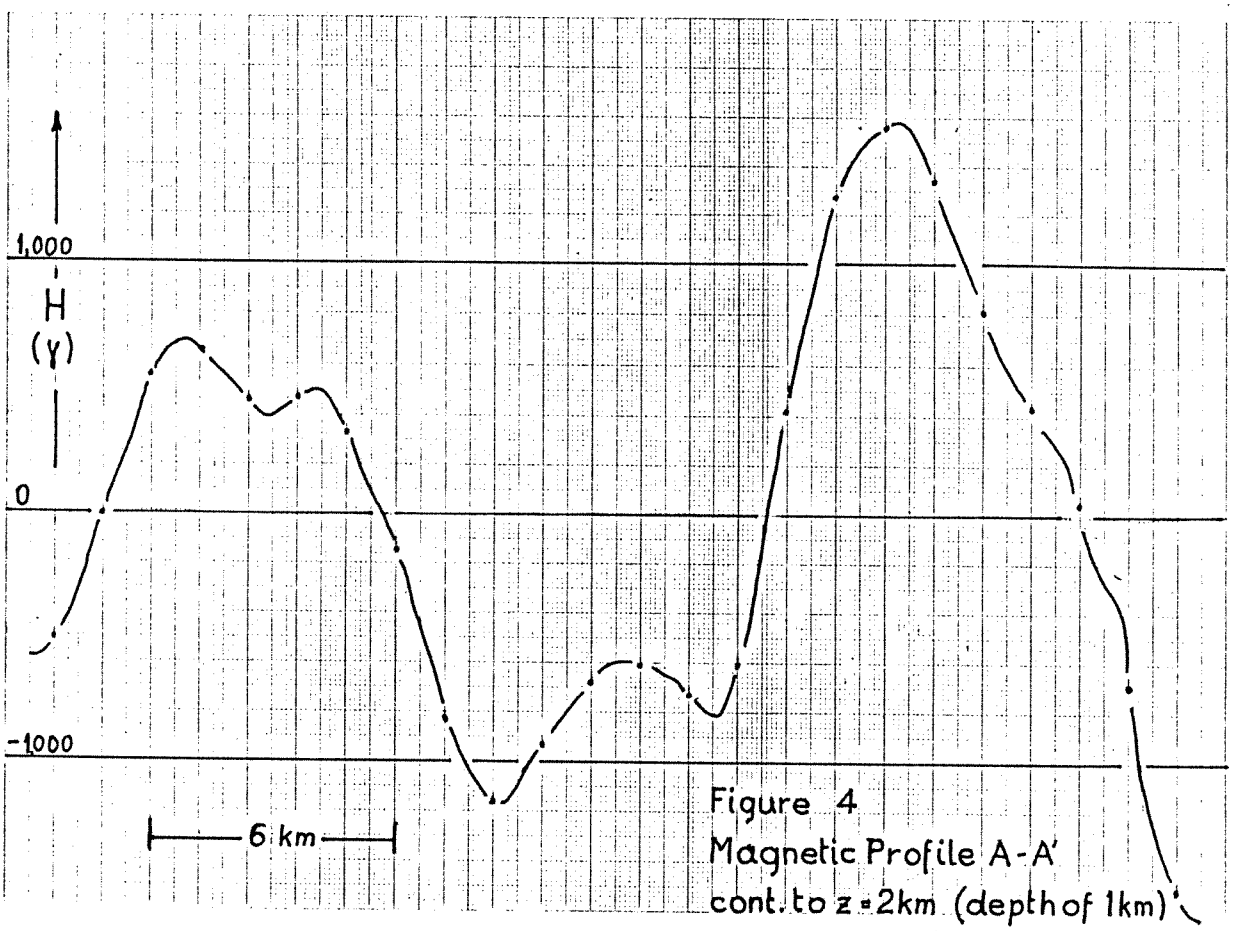

Figure 4
Magnetic Profile A-A'
cont. to z = 2km (depth of 1km)

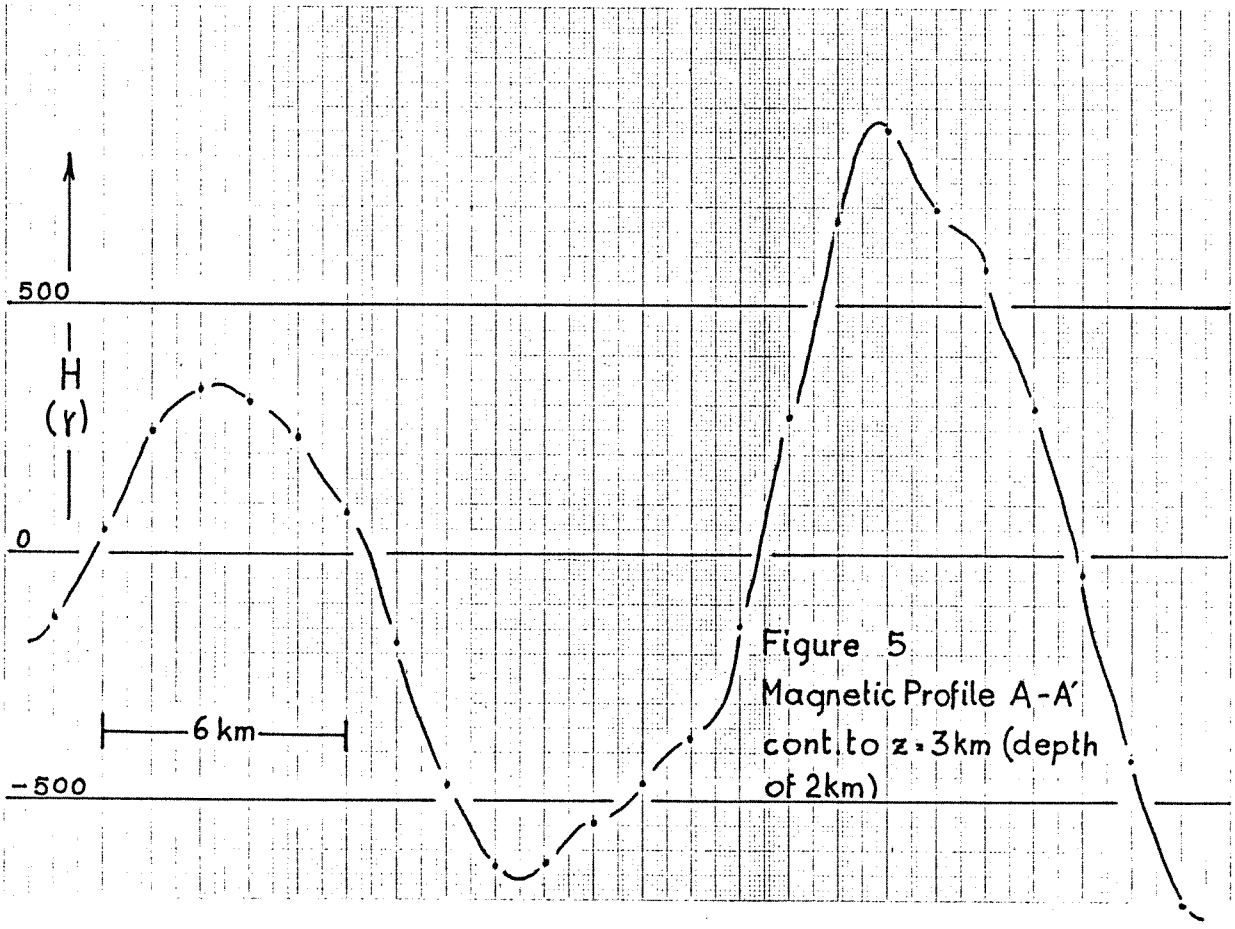

Figure 5
Magnetic Profile A-A'
cont. to z = 3km (depth
of 2km)

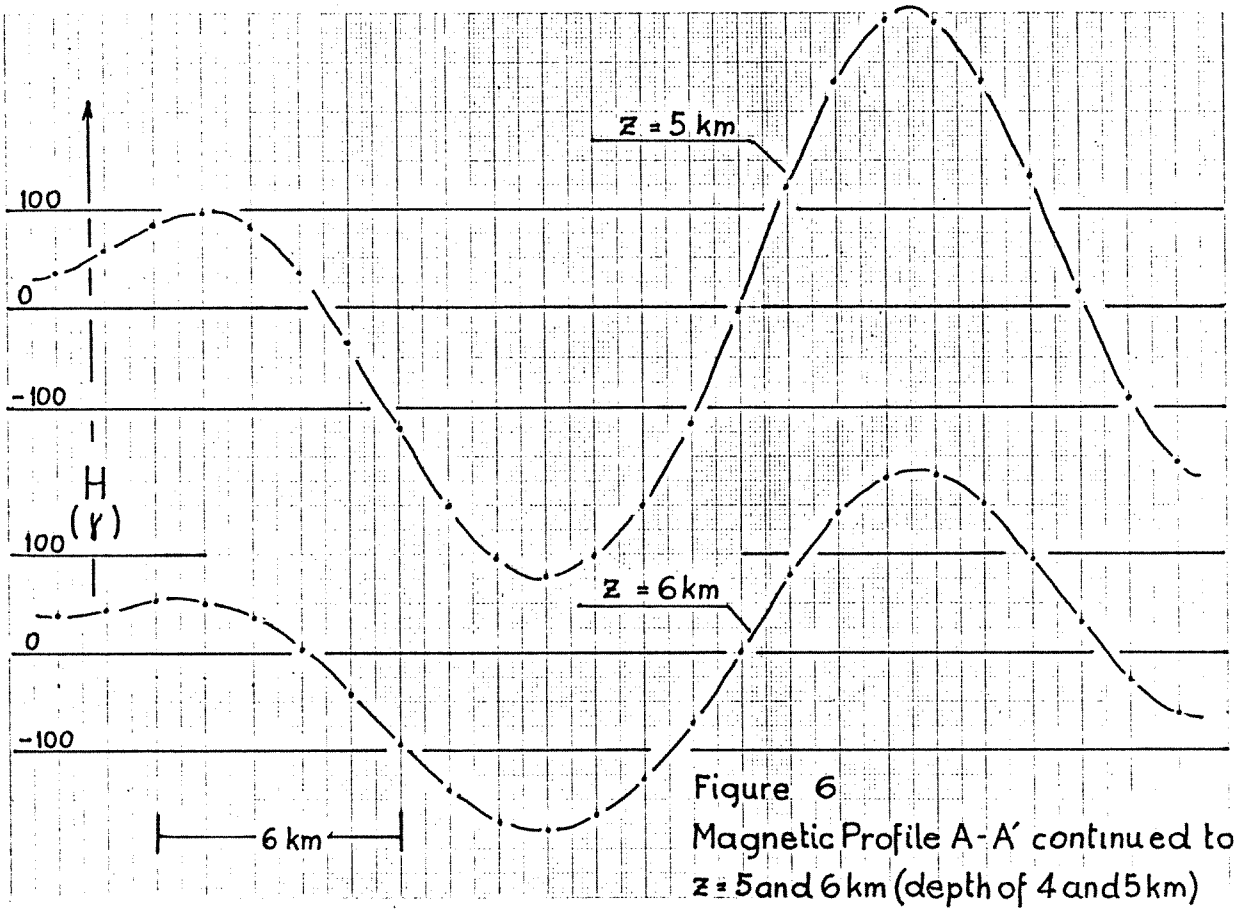

Figure 6
Magnetic Profile A-A' continued to z = 5 and 6 km (depth of 4 and 5 km)

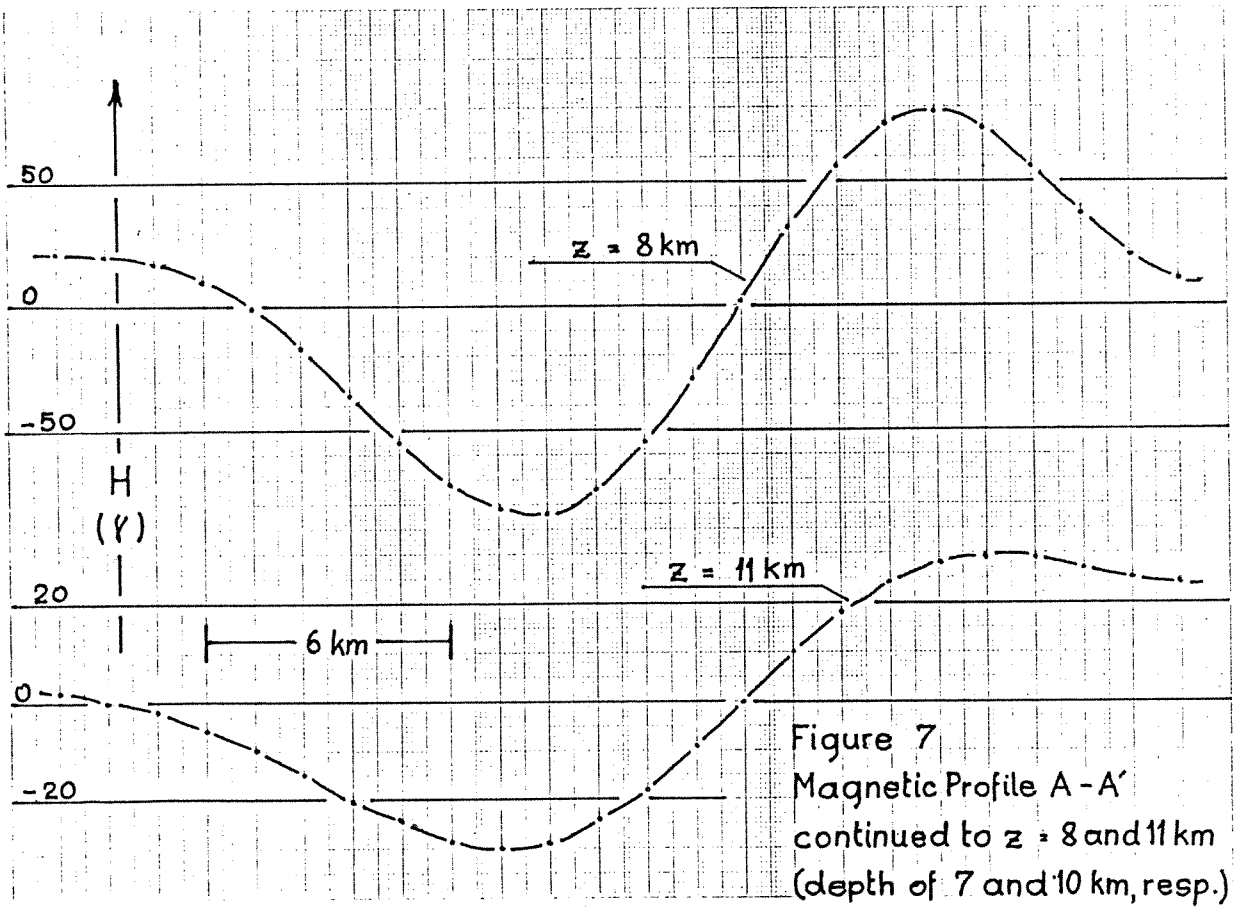

Figure 7
Magnetic Profile A-A'
continued to z = 8 and 11 km
(depth of 7 and 10 km, resp.)

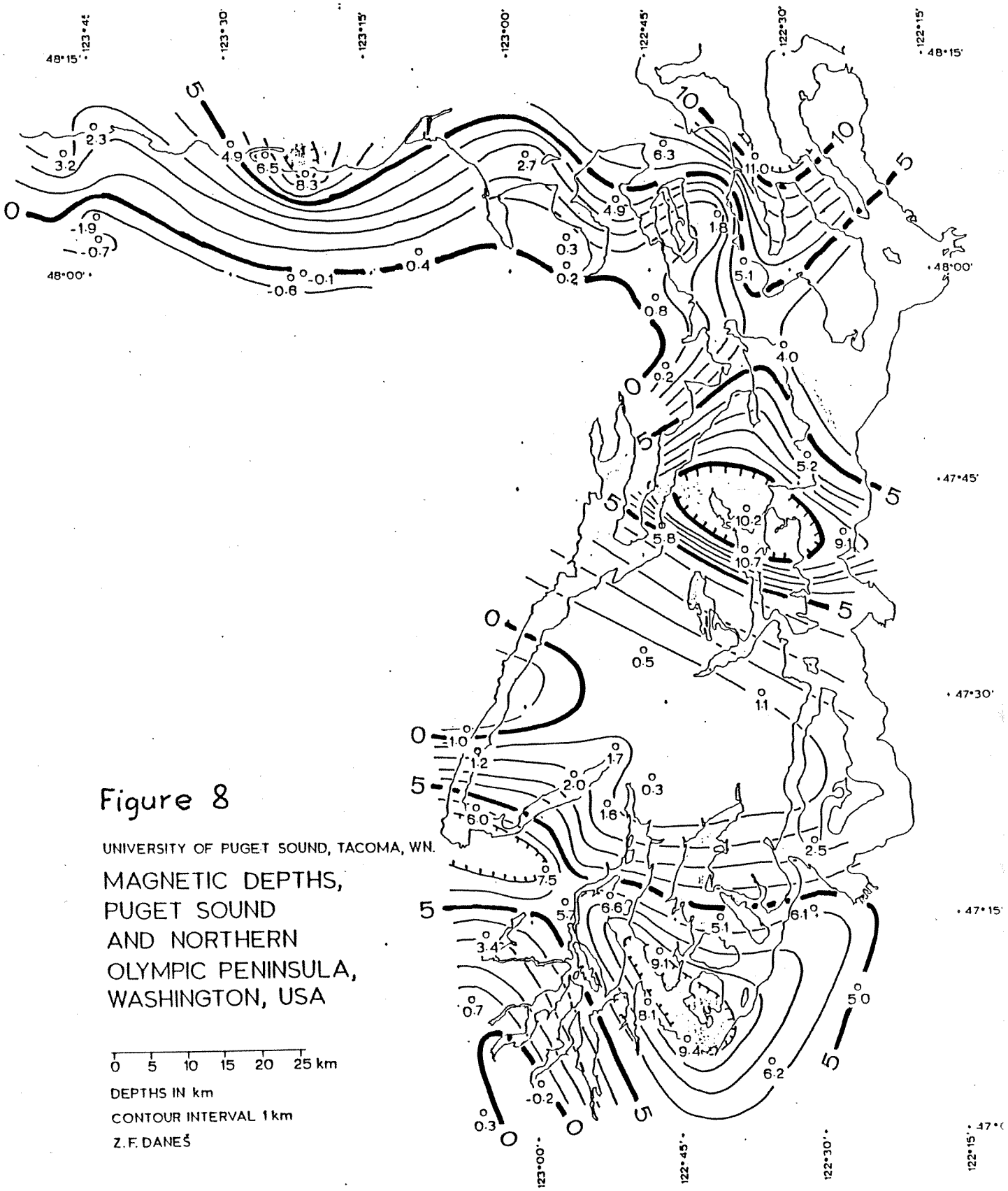

Figure 8

UNIVERSITY OF PUGET SOUND, TACOMA, WN.

MAGNETIC DEPTHS, PUGET SOUND AND NORTHERN OLYMPIC PENINSULA, WASHINGTON, USA

0 5 10 15 20 25 km

DEPTHS IN km

CONTOUR INTERVAL 1 km

Z. F. DANEŠ